Estimating Forces on an Ice Control Structure Using DEM

Steven F. Daly and Mark A. Hopkins
US Army Engineering and Research Center
Cold Regions Research and Engineering Laboratory
72 Lyme Rd, Hanover, NH 03755
Steven.F.Daly@erdc.usace.army.mil
Mark.A.Hopkins@erdc.usace.army.mil

Abstract Recent advances in discrete element modeling now allow the direct simulation of river ice dynamics. By resolving the contact and body forces acting on thousands of individual floes at each time step, the initiation, grounding, and formation of river ice jams can be simulated and studied. The concomitant water flow can be modeled using a coupled unsteady hydraulic model, with feedback provided between floes and water by water drag and blockage of the channel flow area by ice. Four regimes of water flow are modeled: open-channel flow with no ice; flow under moving or stationary ice; high Reynolds number porous flow through grounded and floating ice masses; and flow transported in the interstices of moving ice masses. In this study we investigate the forces exerted by an ice run on a cylindrical pier ice control structure. We initiate an ice run by holding ice at the upstream end of a channel. When the ice is released it is carried downstream by the surge. The ice is stopped by a row of piers placed in a line across the channel. We analyze the time history of the forces exerted by the ice on the piers and the momentum of the moving ice. This allows us to investigate the relationship between the rate of change of momentum and the forces on the piers, channel banks, and bottom. The simulated moments on the ice control structure are compared with results of a similar physical model experiment.

1. Introduction

Ice jams are a wide spread phenomena that can potentially occur in all rivers that form an ice cover during the winter. Ice jams are initiated when the flow stresses the river ice cover causing fractures. This is typically caused by increased flow due to snow melt, rainfall, or release from dams. Further flow increases free the ice cover from the channel banks and transport the ice floes downstream. The ice floes are broken into smaller floes as they are transported and reach a final maximum dimension of roughly three to five times the ice thickness. Ice jams occur at locations where the river's ability to transport the ice floes is exceeded and the motion of the ice floes stops. This can occur at abrupt

decreases in channel slope, sharp bends, natural or man-made channel constrictions, or where an intact river ice cover remains in place. The formation of an ice jam reduces, often dramatically, the conveyance capacity of the river channel for water flow because the jam blocks a portion, or even all, of the flow area of the channel and increases the overall hydraulic roughness of the channel wetted perimeter. This reduction in conveyance increases, often abruptly, the water surface elevation (stage) upstream of the jam. Sudden flooding can result when ice jams form or when they release. The length of an ice jam roughly scales with the length of the upstream reach that contributed ice to the jam, and can vary from tens of meters in small streams to many tens of kilometers in large rivers. In addition to flooding, ice jams can promote bed and bank erosion, remove or damage channel bank vegetation, suspend navigation, and cause extensive damage to river training works and channel bank protection.

Many features of ice jams are poorly understood. There are a number of reasons for this, including their sudden and relatively unpredictable formation, their often short-lived existence, the danger to observers in moving on or about the jam itself, and the difficulties in obtaining information *in situ*. An analytical method for estimating the thickness of an ice jam was developed by Pariset, et al. (1966) by assuming the ice to be a granular material with known material properties, floating in hydrostatic equilibrium, under steady, uniform flow (flow that is unchanging along the channel) conditions. This has been extended to non-uniform but steady flow, and recently, in theory at least, to unsteady flow. The suitability and limitations of the granular assumption as applied to ice jams has been well discussed by Beltaos (1995). Aside from the question of whether or not a moving ice run behaves as a granular mass, the fundamental limitations of the equilibrium models of Pariset, et al. (1966) are the assumptions of hydrostatic equilibrium and the difficulties in moving beyond the steady state analysis. As a result the dynamic forces associated with ice runs and ice jam formation, dominated by the momentum of the arriving ice floes and grounding of the ice jam toe on the channel bottom, cannot be determined. An alternative is the discrete element computer simulation of ice jam formation, in which the fluid drag, contact and body forces acting on each individual ice floes is determined; the river flow is modeled using the dynamic flow equations; and the solution of both is closely coupled through the exchange of information between the two simulations.

This paper describes a series of simulations performed with the coupled river ice model. Ice jams were initiated by at an ice control structure (ICS) in a natural channel. The ICS consisted of 9 cylindrical bridge piers evenly spaced across the channel. (Lever et al 2000) During each simulation the forces acting on the ICS and on the channel sides and bed, the time varying water levels and flow rates, and the ice jam thickness profile were calculated at uniform time intervals. In addition, realistic animations of the ice jam formation process were produced.

2 River Flow Simulation

The channel flow model employs one-dimensional momentum and continuity equations to describe the channel flow. These equations are solved simultaneously for the entire river channel using a four-point implicit discretization scheme (Cunge, et al. 1980). The observation that the ice mass accumulates at the surface of the channel leads naturally to a two-layer description of the channel cross-section. In this two-layer description, the mass of ice is contained in the upper layer. The under ice flow area or lower layer is assumed to be open and unobstructed. In practice the upper layer can extend to the bed when the ice jam grounds on the channel bed or the lower layer can extend to the water surface if no ice is present in a section.

The flow model used in the river flow simulation has been described elsewhere (Daly and Hopkins 1998). The flow in the ice mass, upper layer, and the flow under the ice, lower layer, are considered separately, and then combined to yield one momentum and one continuity equation for each section. The flow rate in each layer is estimated based on the conveyance of the layer. The conveyance is found by making the usual assumption that the conveyance is equal to that of an equivalent steady flow. If the there is no ice present, then the conveyance is

$$K_o = \frac{1}{n_b} A_o R_o^{2/3} \qquad (1)$$

where n_b is the Manning's roughness coefficient of the bed, A_o is the flow area, and R_o is the hydraulic radius. If there is ice present in the section, the flow area and the hydraulic radius must be properly adjusted to account for the presence of the ice floes. The conveyance through the open flow area under the ice will also depend on the relative velocities of the ice and the water. If the ice velocity is less than the water velocity then

$$K_o = \frac{1}{n_c} A_o R_o^{2/3} \qquad (2)$$

where n_c, the composite Manning's n value, is

$$n_c = \left(\frac{n_i^{3/2} + n_b^{3/2}}{2} \right)^{2/3} \qquad (3).$$

Next the conveyance of the flow in the interstitial area of the mass of ice floes is found. The conveyance of the seepage flow K_s, assuming that the flow in the mass of ice floes is high Reynolds number porous flow (Beltaos 1993), is

$$K_s = \lambda A_{ig} \qquad (4)$$

where A_{ig} is the gross cross-sectional area of the mass of ice floes and λ is a seepage coefficient, (Bear 1972) given by

$$\lambda = \sqrt{k_p \frac{e^3}{1-e} g d_s} \qquad (5)$$

where d_s = 6 (volume of floes/area of floes) and k_p is a dimensionless porous flow coefficient. The variable d_s represents the porous medium and is related to the hydraulic radius of the flow in the voids.

The flow model solves for the unknown water surface elevation H and total discharge Q_T at each cross section at every time step. The solution requires two boundary conditions. The prescribed boundary conditions are the discharge at the upstream end of the channel and normal depth at the downstream end of the channel. The system of equations that result from the finite difference form of the continuity and momentum equation applied at each cross section, along with the proscribed boundary conditions, is relatively straightforward to solve using a iterative Newton-Raphson procedure and standard numerical solution techniques.

3 Mechanics of the Ice Model

A discrete element model is a computer program that explicitly models the dynamics of a system of discrete particles. In this simulation the particles are the individual ice floes. The position, orientation, velocity, and shape of each floe are stored in arrays. At each time step, the contact and body forces on each floe are calculated and the floes are moved to new locations with new velocities and orientations that depend on the resultant of the forces. The following brief summary of the mechanics of the particle simulation used in this work is taken from Hopkins and Tuhkuri (1999).

The ice floes in the simulations are flat disks with a circular edge. Two radii R_1 and R_2 define the geometry of the floes. The radius R_1 is the distance from the floe center to the center of the circular edge and R_2 is the radius of the circular edge. The overall diameter d of the floe is $2(R_1+R_2)$ and its thickness h is $2R_2$. Changing R_1 and R_2 can vary the aspect ratio of the floe d/h. The top and bottom surfaces of the floes are flat.

Wherever two floes touch the overlap is interpreted as a deformation of the floes resulting in a contact force. The contact force has components normal and tangential to the surfaces at the point of contact. Forces other than contact forces, such as buoyancy, fluid drag, pressure, etc acting on each floe are also estimated for each floe. The torques on each floe are calculated from the forces and moment arms. After the sum of the forces and torques exerted on each floe has been calculated, the equations of motion for each floe are solved and time advanced. The translational equations of motion use simple central difference approximations. Changes in the angular velocities and orientation of the floes are much more complicated to calculate. Floe orientations are specified by 4 parameters called quaternions (Evans, 1977). Rotational motions are calculated by solving finite difference approximations for the rotational equations of motion expressed in terms of the 4 quaternions. The implementation of this method is described by Walton and Braun, (1993).

In each simulation the change in the kinetic and potential energy of the floes and the energy dissipated by inelastic and frictional contacts and water drag, are calculated at

each time step. Inelastic and frictional dissipation are determined by computing the work performed by the normal and tangential components of each contact force. These calculations are described in Hopkins (1994). The energy balance is used to gauge numerical accuracy. In the simulations described below, the error in the energy balance was less than 2%.

4 Interaction of river flow simulation and ice model

The discrete particle ice model and the channel flow model employ very different approaches in solving their underlying differential equations. In the ice model, the equations of motion for each particle are solved individually and explicitly. The river flow model solves all the equations simultaneously and implicitly. The ice model and the flow model are alternately advanced in time. Information is exchanged between the two models to assure that the solutions are closely coupled. Information regarding the ice floes must be abstracted from the ice model calculations in a form suitable for use by the flow model. The ice information at each cross-section and time step that is passed from the ice model to the flow model includes the bottom elevation of the mass of ice floes, the average porosity of the mass of ice, the mean velocity of the ice, and the mean drag force of the ice on the flow. The information at each cross section and time step that is passed from the flow model to the ice model includes the water surface elevation, the flow rate and flow velocity under the ice, the force of the porous flow acting on the ice, and the differential pressure acting across the ice.

The ice model utilizes the information passed to it by the flow model to estimate all the force acting on each ice particle. The force due to the interaction of floes was described in the previous section. The force of the floes on the bed and banks of the channel are estimated in a similar manner. In fact, the stationary boundaries that form the channel are stationary discrete particles that interact with the ice floes. The water drag force F_d on a floe is given by

$$\vec{F}_d = -\tfrac{1}{2} C_d \rho_w A \vec{V} \left| \vec{V} \right| \qquad (6)$$

where C_d is the drag coefficient, ρ_w is the water density, and $A=\pi(R_1+R_2)^2$ is the floe area. The drag force is separated into components normal and tangential to the flat surface of a floe. The drag coefficient C_d, based on floe area, is 1.17 for flow normal to the flat surface and 0.1 for flow tangential to the flat surface (White, 1979). The flow is assumed to be turbulent. The water drag is applied only to the underwater floes that are in an exposed position. Floes in the interior of a moving mass of floes feel no drag. The drag force and its moment due to porous flow are applied to each floe. The buoyant force and its moment on each floe are calculated. The gravity force on each flow is calculated. This force can exert no moment on a floe. The differential pressure force due to the slope of the water surface is also estimated and applied to each submerged floe.

5.Variable Channel Geometry

Earlier, we (Daly and Hopkins, 1998) simulated river ice jam formation in uniform, rectangular channels. In the present work, the ice model uses variable cross-sectional channel geometry, while the hydraulic model uses equivalent rectangular cross sections. The riverbed used in the current simulations is shown in Figure 1. The model riverbed was obtained from survey data used by Lever et al (2000) for their model study of the Cazenovia Creek (Buffalo, NY) ice-control structure (ICS). The nine cylindrical piers at the lower end of the channel form the ICS. The riverbed was implemented in the ice DEM by reinterpolating the surveyed river cross sections at regular 3-m intervals,

triangulating the area between adjacent cross sections, and making each triangular section into a discrete element that can interact with and confine the ice floes within the channel.

6. Estimation of the Ice Porosity and Thickness

The porosity and thickness of the ice mass at each section are important components of the feedback from the ice DEM to the hydraulic model. The porosity of the ice mass is used to determine the seepage coefficient of the ice mass. The thickness is required to determine the overall area of ice that is available for seepage flow and the area beneath the ice mass that is available for under-ice flow. The porosity of the entire ice mass and the overall ice mass thickness in each cross-section where ice is present are calculated by dividing the cross section into transverse subsections. First, the elevation of the mean top surface $Z_{\max j}$ and bottom surface $Z_{\min j}$ of the ice floes in each subsection j are calculated. The volume contained between the mean top and bottom surfaces of section i, called $V_i^{'}$, is

$$V_i^{'} = \sum_j \Delta x \Delta y (Z_{\max j} - Z_{\min j}) \tag{7}$$

where j denotes the subsection of cross section i, Δx is the section length, and Δy is the subsection width. The actual volume of ice V_i in cross-section i is

$$V_i = \sum_j \sum_k V_{jk} \tag{8}$$

where V_{jk} is the volume of floe k whose center lies in cross section i and subsection j. The porosity e_i in cross section i is

$$e_i = \frac{V_i^{'} - V_i}{V_i^{'}} \tag{9}$$

The elevation of the bottom surface of the ice in a rectangular cross section is used by the hydraulic model to divide the flow in a cross-section into an under-ice open water part and a through-ice porous flow part. The elevation of the bottom surface of the ice in section i, called ibp_i is

$$ibp_i = Z_{bed-i} + \frac{\sum_j n_j (Z_{\min - j} - Z_{bed-j})}{\sum_j n_j} \tag{10}$$

where Z_{bed} is the bed elevation and n_j is the number of floes in subsection j.

7. Simulation of an Ice jam at the Cazenovia Creek ICS

We began the simulation by feeding ice floes, one at a time, into the upper end of the channel shown in Figure 1. We placed a temporary "virtual" barrier across the channel 335 m above the ICS to catch the ice. We constructed samples with approximately 8000 floes at equilibrium behind the temporary barrier. The parameters used in the simulations are shown in Table 1.

Table 1. Parameters used in the river ice jam simulations.

Parameter	*Value*
channel length	830 m
Manning's n	0.03
channel slope	0.001
floe diameter	2.6 m
floe thickness	0.6 m
upstream discharge	44 $m^3 s^{-1}$
pier spacing	5.2 m
pier diameter	1.5 m
ρ_i (ice density)	900 kg m^{-3}
ρ_w (water density)	1000 kg m^{-3}
μ (ice/bed friction)	0.6
μ (ice/ice friction)	0.3
k_n (normal contact stiffness)	10^6 N m^{-1}
k_p (porous flow parameter)	0.7

The dimensions of the channel, floes, and piers were taken from Lever et al (2000) as were measurements made during physical model tests of the moment on the structures. We estimated the ice/bed and ice/ice friction coefficients on the basis of previous experience. The value of the porous flow parameter k_p was taken from Beltaos (1995). The normal contact stiffness k_n was sufficient to keep the nominal maximum overlap in floe–floe contacts at an acceptable level of about 1% of the floe diameter.

The initial configuration is shown in Figure 2. The head loss through the initial jam was almost 3 m. After the hydraulic conditions in the channel reached near equilibrium, the "virtual" barrier was removed. The ice at the downstream end of the accumulation began moving immediately thereafter. Because the ice behind the leading floes must wait for the leading floes to move, the thick toe of the jam thins and stretches.. The leading floes cover the 335-m distance to the ICS in about 140 s. Arching between the piers of the ICS begins as soon as the first floes reach the ICS. As the initial floes arch, the following floes pile into them, rapidly enlarging the jam. The momentum of the following floes causes the jam to thicken and ground. A positive wave is created that travels upstream. This wave increases the depth of flow and reduces the flow in the channel. The jam at the ICS is shown in Figure 3.

The hydrograph from the formation of the jam are shown in Figure 4. The stages follow those recorded in the physical model test in broad outline (Lever et al., 2000). The

increase in stages following the release of the "virtual" barrier can be seen for the locations downstream of the barrier (the distances -90 m, +3 m, +330 m are measured relative to the ICS location), as well as the decrease for the location upstream of the "virtual" barrier (+388m). The initial wave of water that reaches the structure ahead of the ice mass can be clearly seen at locations upstream and downstream of the ICS (+3 m , -90 m). The positive wave that travels upstream can also be clearly seen at the two most upstream locations (+330m, +388m) at time 260 s.

The overturning moments acting on the ICS are shown in Figure 5 for both the DEM (sim) and the physical model tests (mod) (Lever et al 2000). Shown are the moments about the transverse axis caused by the stream-wise forces averaged over five of the piers. The magnitude of the moments calculated by the DEM and measured in the physical model tests compare quite well.

All the forces acting on the ice mass over the course of the simulation are shown in Figure 6. These forces include the force exerted by the ICS piers, the force exerted by the bed (including banks), the fluid drag force, the drag force from the porous flow, and the differential pressure force. Also shown is the change in momentum of the ice, and the residual, which is the difference between the sum of all the forces acting on the ice and the change in momentum of the ice. The residual can be seen to be small throughout the simulation. The initial acceleration of the grounded ice mass after the "virtual" barrier is removed is driven by the differential pressure force and resisted by viscous drag. The change in momentum is positive when the ice is initially accelerated and becomes negative when the ice decelerates upon striking the ICS. The force on the piers of the ICS increases during this period of deceleration. The force on the bed and banks also reaches a maximum during this period. The force on the bed gradually decreases after jam formation relecting the decrease in the viscous drag and differential pressure forces that may be caused by the wave traveling upstream, which raises the water level and tends to lift the ice off the bed.

7. Summary

The work described in this paper further extends our ability to model ice jams by addressing the case of ice jams in natural channels. The DEM simulation of the dynamic ice motion has no lower limit on ice concentration, or any requirements with regard to hydrostatic equilibrium of the ice mass. As a result, a wide range of ice conditions can be simulated, including grounding of the ice jam on the channel bed. The one-dimensional flow model can also simulate a wide range of flow conditions, including high-Reynolds-number seepage flow through a grounded ice mass. A further advantage of this approach is the ability to extract detailed, time-varying information from the simulation, including water levels, flow rates, ice jam thickness, and forces. Realistic animations of ice jams can be produced and viewed from any vantage point. These results suggest the importance of understanding the relationship between porous flow, the dynamic interaction of moving ice, and the creation of waves in response to the formation of the jams.

7. References

Bear, J. (1972) *Dynamics of Fluids in Porous Media*, Dover, New York.

Beltaos, S. (1993) Flow through breakup jams, Proc. 11th Canadian Hydrotechnical Conference, Fredericton, NB, June 8-11, 1993.

Beltaos, S. (ed.) (1995) *River Ice Jams*. Water Resources Publications.

Cunge, J.A., F.M. Holly, and A. Verwey (1980) *Practical Aspects of Computational River Hydraulics*. Institute of Hydraulic Research, College of Engineering, The University of Iowa, Iowa City.

Daly, S.F., and M.A. Hopkins (1998). Simulation of river ice jam formation. In Ice in Surface Waters, Proceedings of the 14th International Symposium on Ice, 27–31 July, Potsdam, New York (H.H. Shen, Ed.). Balkema.

Evans, D.J. (1977) On the representation of orientation space. Molecular Physics, 34(2): 317–325.

Hopkins, M.A., and J. Tuhkuri, (1999) Compression of floating ice fields, J. Geophys. Res., 104, C7, 15,815-15,825

Hopkins, M.A., (1994) On the ridging of an intact sheet of lead ice, J. Geophys. Res., 99, C8, 16351-16360

Lever, J.H., G. Gooch, and S.F. Daly (2000) Cazenovia Creek Ice-Control Structure, TR-00-14, Engineer Research and Development Center, Cold Regions Research and Engineering Laboratory, Hanover, NH.

Lever, J.H., G. Gooch, A. Tuthill and C. Clark, (1997) Low-cost ice-control structure, J. Cold Regions Engineering, ASCE, 11(3), 198–220.

Pariset, E., R. Hausser, and A. Gagnon (1966) Formation of ice covers and ice jams in rivers. Journal of Hydraulics Division, 92(HY6): 1–24.

Walton, O.R. and R.L. Braun, 1993, Simulation of rotary-drum and repose simulations for frictional spheres and rigid sphere clusters, Joint DOE/NSF Workshop On FLOW OF PARTICULATES AND FLUIDS, Sept. 29 Oct. 1, 1993, Ithaca, NY.

White, F.M., 1979, Fluid Mechanics, McGraw-Hill, New York.

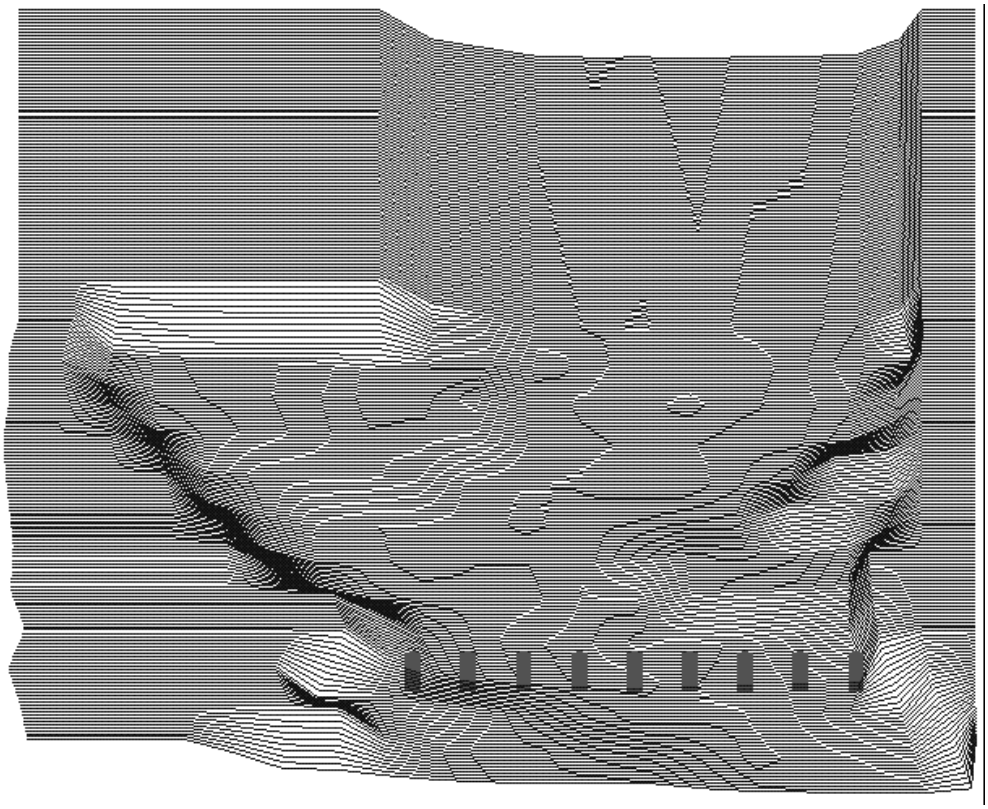

Figure 1. Channel geometry

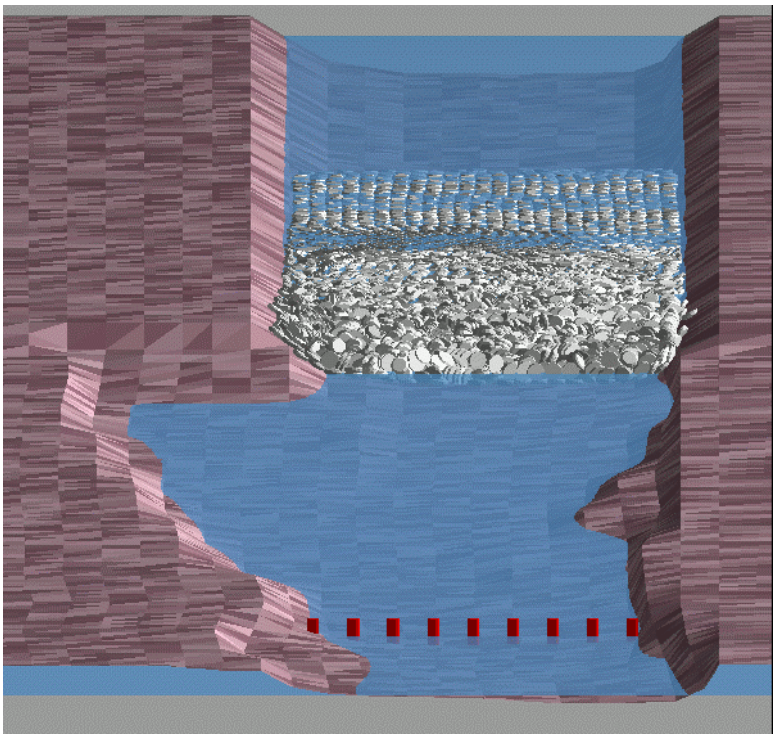

Figure 2. Initial ice conditions

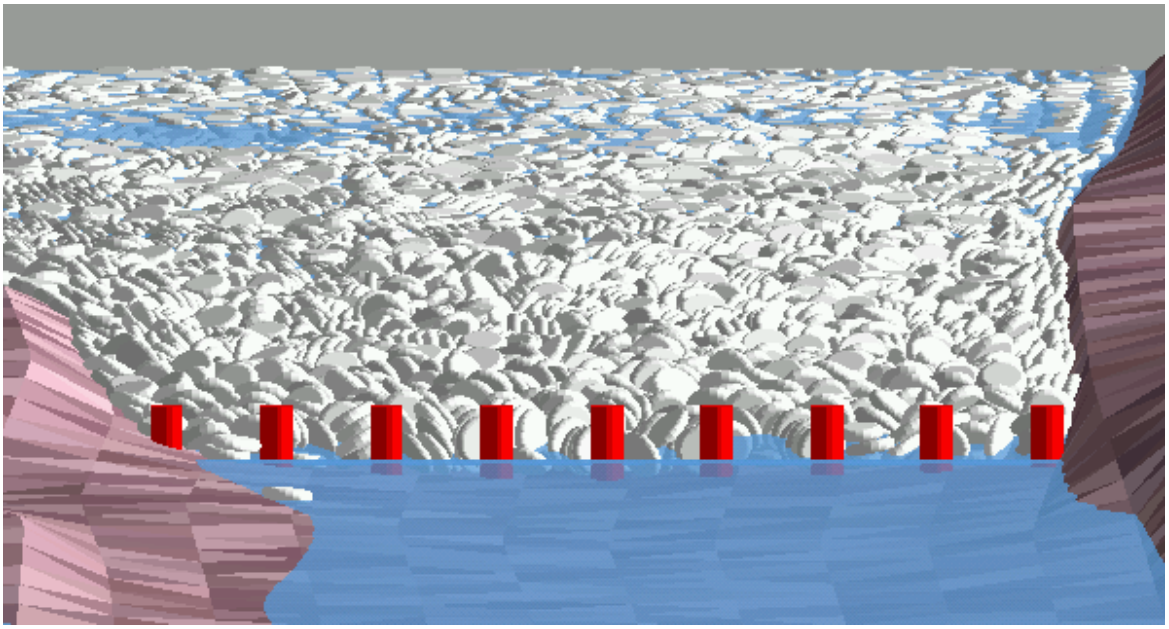

Figure 3. Ice jam at the ice control structure

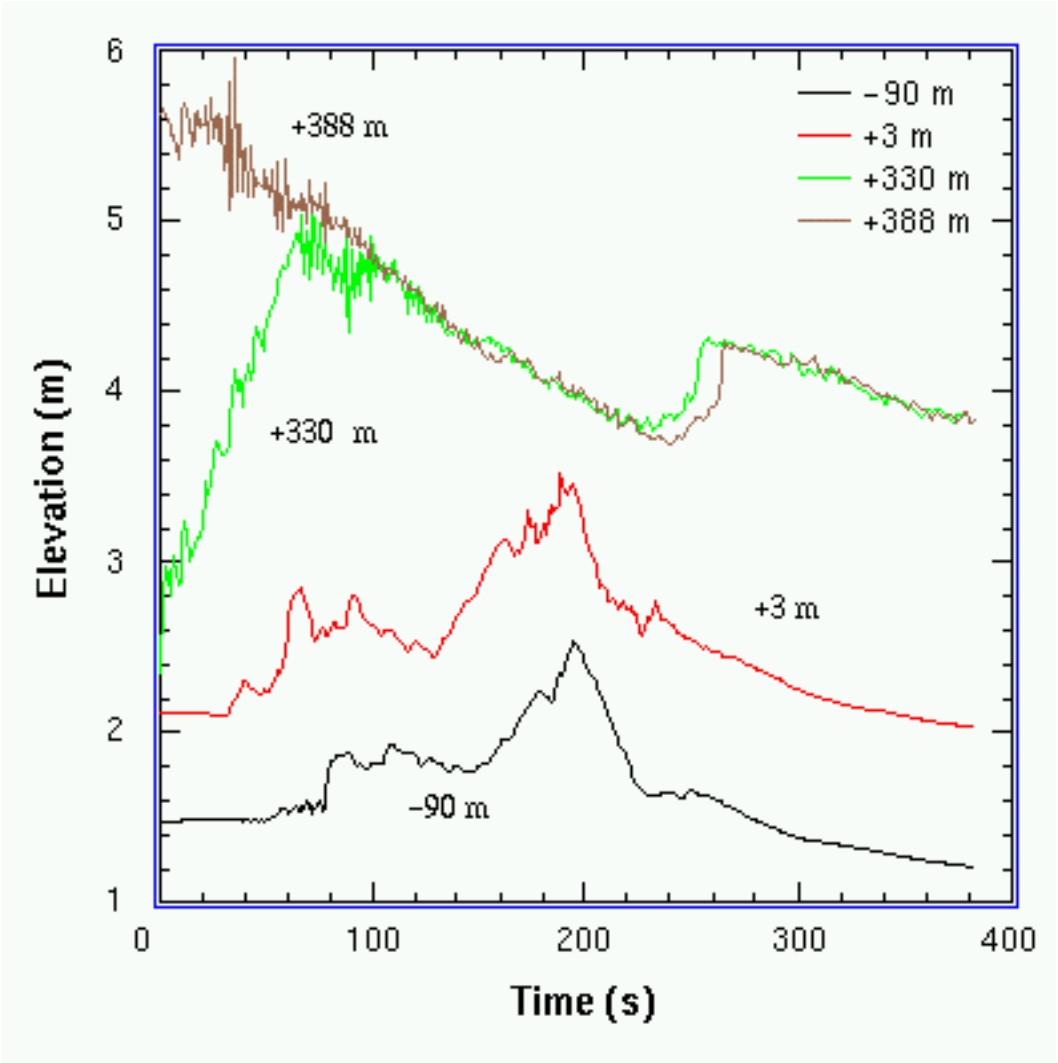

Figure 4. Hydrographs. -90m: downstream of ICS, +3m: immediately upstream of ICS; +330m: downstream of "virtual" ice barrier; +388m: upstream of "virtual" ice barrier

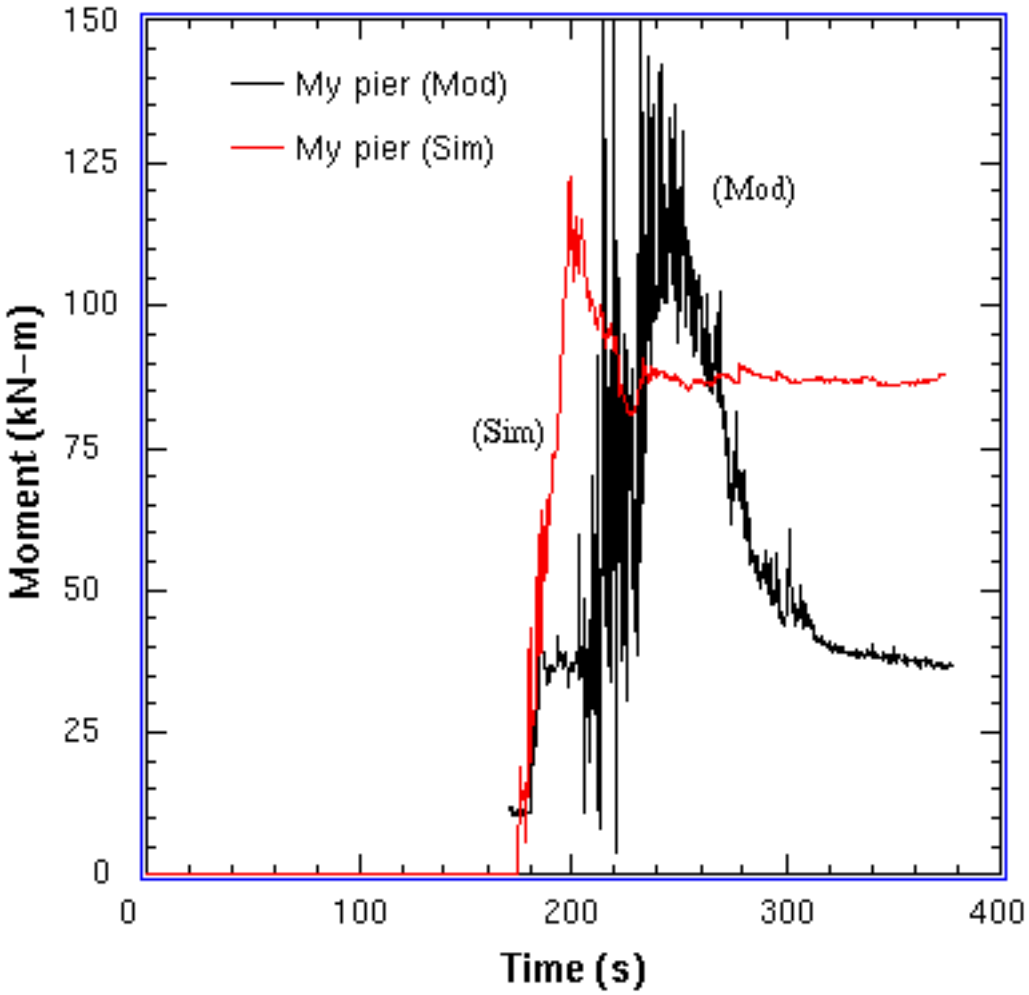

Figure 5. Moments on ICS

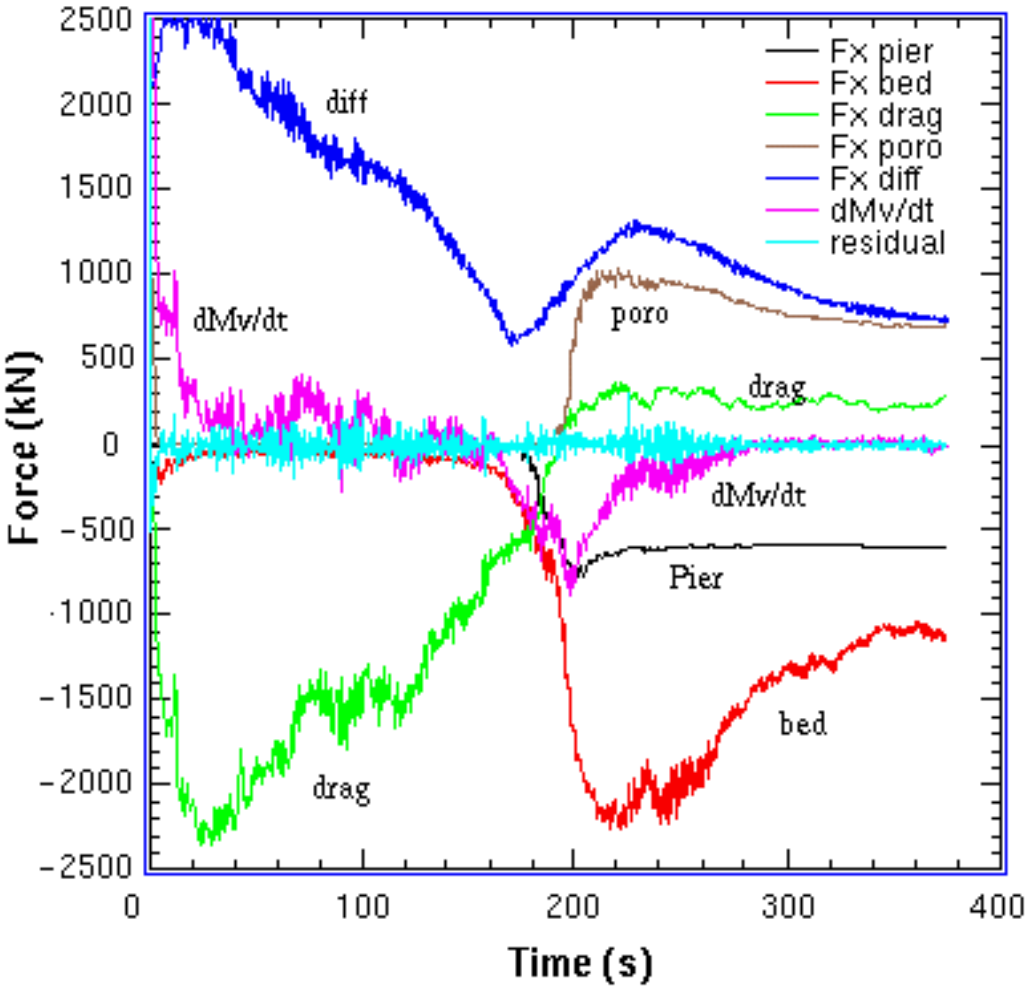

Figure 6. Forces acting in simulation